

Master's Thesis

Title

**Parameter tuning of end-to-end bandwidth measurement method
with power-saving routers**

Supervisor

Professor Hirotaka Nakano

Author

Daisuke Kobayashi

February 14th, 2012

Department of Information Networking
Graduate School of Information Science and Technology
Osaka University

Master's Thesis

Parameter tuning of end-to-end bandwidth measurement method
with power-saving routers

Daisuke Kobayashi

Abstract

The increase in energy consumption associated with network traffic explosion is becoming a major problem. To realize energy-efficient networking, a number of researchers have focused on technologies that dynamically adjust the processing performance and the link speed of routers and switches according to the network traffic load. However, when such power-saving routers and switches are present in the network, the existing network protocols and control methods may not work well since they do not assume the existence of such routers and switches. The author focuses on the measurement method of an end-to-end available bandwidth, which is an important performance metric for various network controls.

In this thesis, the author introduces a parameter tuning method for Pathload, which is a popular tool for measuring the end-to-end available bandwidth, to maintain the measurement accuracy in the network with power-saving routers, while not affecting the behavior of power-saving routers. For that purpose, the author first investigates the interactions between the bandwidth measurement behavior of Pathload and the energy efficiency of power-saving routers by conducting extensive simulation experiments. In the simulation experiments, the author examines the effects of the power-saving router on the measurement accuracy and the effects of the Pathload measurement on the behavior of the power-saving router. Based on simulation results, the author exhibits that both the measurement accuracy of Pathload and the energy efficiency of power-saving routers degrade, particularly when the power saving functions are triggered in short cycles.

As the second contribution of this thesis, the author proposes a parameter tuning method for Pathload that maintain measurement accuracy without affecting the behavior of power-saving routers. The author accomplishes this by giving simple mathematical analysis of the traffic load of

Pathload on the power-saving router. The author confirms the accuracy of our analysis by comparing the analysis results with corresponding simulation results. The author also shows that Pathload can measure an available bandwidth without affecting the behavior of power-saving routers by tuning the number of probing packets on the basis of the analysis results.

Keywords

Available Bandwidth

Bandwidth Measurement

Active Probing

Energy Efficiency

Router

Contents

1	Introduction	6
2	Interactions between Pathload’s measurement and power-saving routers	8
2.1	Power-saving router model	8
2.2	Pathload algorithm	9
2.3	Effect of the measurement on power-saving routers	10
2.4	Effect of changing bandwidth on the measurement	10
3	Performance evaluation of Pathload with a power-saving router	13
3.1	Simulation settings	13
3.2	Behavior of the power-saving router	16
3.3	Measurement accuracy of Pathload	21
4	Parameter tuning of Pathload for not affecting a power-saving router	23
4.1	Conditions for not affecting a power-saving router	23
4.2	Verification	26
5	Conclusions and future works	29
	Acknowledgement	30
	Reference	31

List of Figures

1	Measurement process of Pathload	12
2	Network topology for simulation experiments	14
3	Change in the utilization of the tight link	17
4	Change in the physical bandwidth of the tight link	18
5	Effect of the maximum bandwidth of the tight link on the utilization changes . . .	19
6	Effect of the maximum bandwidth of the tight link on the physical bandwidth changes	20
7	Measurement results obtained with Pathload	22
8	Relationship between packet stream length and monitoring interval	25
9	Effect of the number of packets of per packet stream on the utilization changes .	27
10	Effect of the number of packets of per packet stream on the physical bandwidth changes	28

List of Tables

1	Parameters of power-saving router	15
2	Parameters of Pathload	15

1 Introduction

The increase in energy consumption in computer networks associated with the constant intensification of network traffic is becoming a major problem. According to the estimation by Ministry of Economy, Trade and Industry (METI), the total power consumption of network equipment in Japan will increase to 5 times, from approximately 5 billion kWh of 2006 to 25 billion kWh of 2025 [1]. Many researchers are studying methods for energy-efficient networking by introducing power-saving routers and switches which adjust their processing performance and link speed according to the network traffic load. For example, a power saving method for Gigabit Passive Optical Network (G-PON) was introduced [2] in which routers adjust their link speed to either 1 Gbps or 10 Gbps and enter sleep mode according to the network traffic load. Power saving techniques for Ethernet adapters with adaptive link rates [3], ADSL2 and ADSL2+ [4] have also been proposed.

However, when power-saving routers and switches are present in the network, the existing network protocols [5–11] and control methods [12–16] may not work well since they do not assume the existence of such mechanisms. For example, recent versions of Transmission Control Protocol (TCP) [17] in Windows and Linux, so-called delay-based congestion control mechanisms are employed to enhance the data transmission performance [18, 19]. They monitor the round trip times (RTTs) of the TCP connection to regulate the congestion window size, that implicitly assumes the fixed physical bandwidth. Therefore, the existence of power-saving routers that dynamically change their physical bandwidth would degrade the data transmission performance of such TCP connections. One possible way to solve this problem is to measure the available bandwidth itself of the TCP connection [20, 21]. In this thesis, therefore, the authors focus on the measurement method of the end-to-end available bandwidth.

Numerous tools for measuring end-to-end available bandwidth have been developed, such as Pathload [22], ImTCP [23], and others [24–37]. However, these tools do not take into account environments where the physical link bandwidth changes according to the network load. Furthermore, since most measurement methods involve sending probing packets at an extremely high rate, the energy efficiency of power-saving routers may degrade, since power-saving routers increase its physical link bandwidth to accommodate the traffic load by bandwidth probing.

In this thesis, as a first step toward tackling the above problems, the author investigates the in-

interactions between the bandwidth measurement behavior of Pathload and the energy efficiency of power-saving routers by conducting extensive simulation experiments. For the simulation experiments, the author introduces the model of the power-saving router proposed in [38] and describes the Self-Loading Periodic Streams (SLoPS) measurement algorithm utilized by Pathload. In the simulation experiments, the author examines the effects of the power-saving router on the measurement accuracy of Pathload and the effects of the Pathload measurement on the behavior of the power-saving router under various settings of power-saving routers.

The author then proposes a parameter tuning method for Pathload that maintain the measurement accuracy without affecting the behavior of power-saving routers after giving simple mathematical analysis of the traffic load of Pathload on the power-saving router. The author shows that tuning the number of probing packets on the basis of the analysis results enables Pathload to measure without affecting the behavior of power-saving router. The author also confirms the accuracy of our analysis by comparing the analysis results with corresponding simulation results.

The rest of this thesis is organized as follows. Section 2 discusses the interactions between the Pathload and power-saving routers after providing an overview of power-saving routers and Pathload algorithm. In Section 3, the author evaluates the performance of Pathload in a network environment with power-saving routers by simulation experiments and the energy efficiency of power-saving routers. Section 4 provides guidelines in terms of a parameter tuning method for Pathload based on mathematical analysis. Finally, the author concludes this thesis and presents goals for future work in Section 5.

2 Interactions between Pathload's measurement and power-saving routers

2.1 Power-saving router model

In this subsection, a model for a power-saving router, which regulates its physical link bandwidth according to the network traffic load, is presented. The model is constructed based on the power-saving router architecture proposed in [38].

It is assumed that the power-saving router monitors its link utilization at regular intervals (of the order of milliseconds to seconds) and regulates its physical bandwidth according to the observed utilization. The maximum value of the physical link bandwidth, in other words, the link bandwidth without power saving, is denoted as C_{max} . Assuming an N -level stepwise power saving configuration, the i th setting of the physical bandwidth, denoted as C_i , is defined as follows.

$$C_i = \frac{i}{N} C_{max} (1 \leq i \leq N) \quad (1)$$

τ is utilized to represent the length of the interval for monitoring link utilization and assumes that the power-saving router changes the link bandwidth at the same cycle. $P(t)$ and $C(t)$ represent the amount of traffic observed at the link and the physical link bandwidth at t th time slot, respectively. In this case, the link utilization $u(t)$ is represented as follows.

$$u(t) = \frac{P(t)}{C(t)\tau} \quad (2)$$

The average link utilization $U(t)$ at the t th time slot is expressed as an exponential moving average.

$$U(t) = (1 - w)U(t - 1) + wu(t) \quad (3)$$

The parameter w in Equation (3) is the averaging weight. The power-saving router determines the physical link bandwidth at the $(t+1)$ th time slot according to the following equations.

$$C(t + 1) = \begin{cases} C_{i+1} & \text{if } U(t) \geq \lambda_u \text{ and } i < N \\ C_{i-1} & \text{if } U(t) \leq \lambda_l \text{ and } i > 1 \\ C_i & \text{otherwise} \end{cases} \quad (4)$$

The parameters λ_u and λ_l in Equation (4) are thresholds of the link utilization which are used to determine whether the power-saving router should increase or decrease its physical link bandwidth, respectively. From Equation (4), it follows that the power-saving router increases its physical link bandwidth when the average link utilization becomes larger than λ_u and decreases the bandwidth when the average link utilization becomes smaller than λ_l .

2.2 Pathload algorithm

Next, the SLoPS measurement algorithm utilized by Pathload is explained. The sender sends packet streams to the receiver at a certain rate. As the receiver observes the intervals at which packets in the streams arrive, it compares the intervals with the corresponding sending intervals determined by the sender and estimates the available bandwidth. Finally, the sender adjusts the sending rate of subsequent packet streams according to the observation results provided by the receiver. This cycle is repeated until the algorithm obtains an estimate of the available bandwidth. The packet streams sent in every cycle are referred to as a *fleet*.

Pathload maintains upper and lower bounds of possible values for the available bandwidth of the end-to-end path and updates these values according to the packet arrival intervals observed by the receiver. $R_{max}(f)$ and $R_{min}(f)$ is denoted the upper bound and the lower bound at the f th cycle. In this case, the sender determines $R(f)$, which is the sending rate of a packet stream in the f th cycle, as follows.

$$R(f) = \frac{R_{max}(f) + R_{min}(f)}{2} \quad (5)$$

The initial value of $R_{min}(0)$ is 0 bps, and $R_{max}(0)$ is determined based on rough estimation of the upper bound of the available bandwidth [39].

When $R(f)$ and the packet size L are given, the sending interval $T(f)$ of packets in packet streams in the fleet of the f th cycle is calculated as follows.

$$T(f) = \frac{L}{R(f)} \quad (6)$$

The length of the packet stream in the fleet of the f th cycle, denoted as $V_S(f)$, is represented as follows by using Equation (6) and K , which is the number of packets contained in each packet

stream.

$$\begin{aligned} V_S(f) &= KT(f) \\ &= \frac{KL}{R(f)} \end{aligned} \quad (7)$$

Note that $V_S(f)$ represents the temporal length of a packet stream in the f th cycle traversing the power-saving router.

2.3 Effect of the measurement on power-saving routers

Here, the behavior of power saving router is discussed when Pathload measures the available bandwidth of the path traversing the router. Assuming that $K = 100$ and $L = 1500$ bytes, which is the standard setting of Pathload, a packet stream for each measurement cycle carries 150 Kbytes of probe packets. It corresponds to 12 ms when $R(f) = 100$ Mbps. Since Pathload makes sending interval between packet streams enough long for the purpose of avoiding excess possession of bandwidth, multiple packet streams do not interfere each other. However, it is assumed that in the power-saving router proposed in [38], the interval for monitoring link utilization of the power-saving router is the order of milliseconds. Therefore, it is expected that the power-saving router changes the physical bandwidth to accommodate the probe traffic by Pathload. This is because the link utilization of the power-saving router approaches 100 % when a packet stream passes through the link of the router, especially when an actual available bandwidth of link is small.

The above behavior is caused by the algorithm of Pathload, where $R(f)$ approaches the actual available bandwidth of the end-to-end network path, which is the nature of SLoPS algorithm described in Section 2.2. In addition, the longer the length of the packet stream, the longer time of occupying the available bandwidth of the power-saving router. The length of the packet stream depends on both K and $R(f)$, which described in Equation (7). From Equation (7), it is observed that the length of a packet stream becomes long when an actual available bandwidth of the end-to-end network path becomes small, since $R(f)$ becomes small when an actual available bandwidth becomes small.

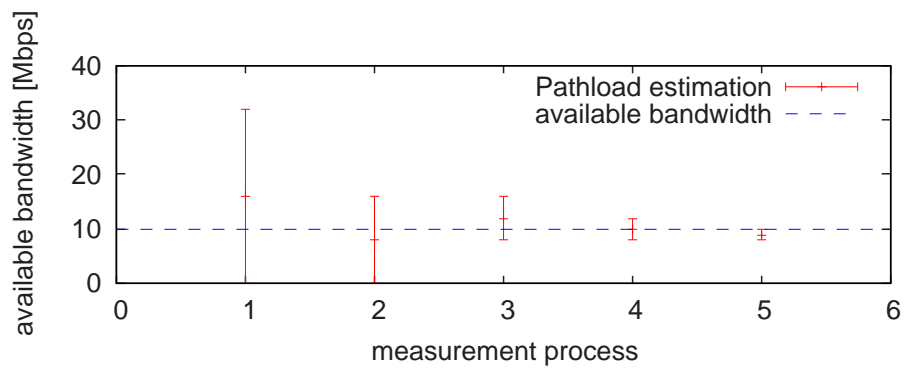
2.4 Effect of changing bandwidth on the measurement

Finally, the author describes the behavior of Pathload's measurement when the power-saving router changes its physical link bandwidth. For that purpose, the author shows numerical cal-

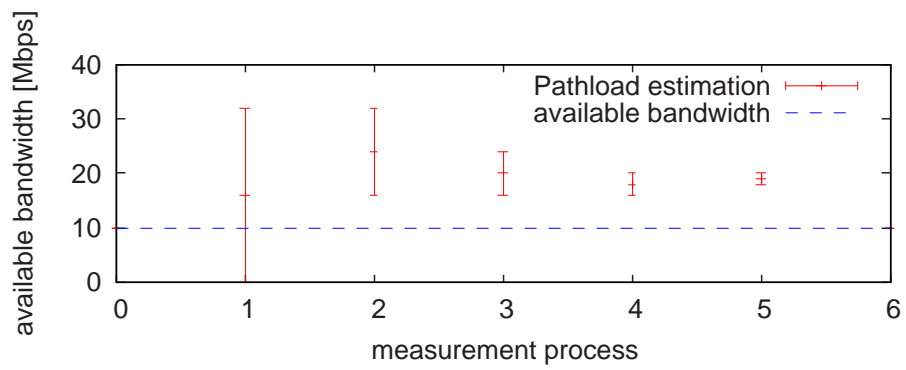
calculation results of Pathload algorithms, assuming that a power saving router exists on the path. In Figures 1(a) and 1(b), Pathload's measurement process based on SLoPS algorithm is depicted. In these figures, the vertical axis represents the available bandwidth and the horizontal axis represents the measurement process in estimating available bandwidth by Pathload. In both figures, it is assumed that Pathload finishes estimating and gives result at the 5th measurement process. The true value of the available bandwidth is set to 10 Mbps. In Figure 1(a), the author assumes that the power-saving router does not change its physical bandwidth during the measurement and calculate the change in the upper and lower bounds of available bandwidth estimated by Pathload. On the other hand, in Figure 1(b), the author assumes the situation where the power saving router increase its physical bandwidth at the first process of Pathload measurement, and the available bandwidth based on the increased physical bandwidth becomes 20 Mbps.

From Figure 1(a), it is observed that Pathload measures the available bandwidth successfully. On the other hand, in Figure 1(b), Pathload measures the available bandwidth based on the increasing physical link bandwidth, which is NOT a correct estimation since the available bandwidth was 10 Mbps when the measurement started. Such degradation of the measurement accuracy occurs when the power-saving router increase its physical bandwidth due to increased traffic load by the measurement itself.

As described above, Pathload's measurement accuracy significantly degrades when the power-saving router changes its physical bandwidth during the measurement. Furthermore, such phenomena also degrade the energy efficiency of power-saving routers since the change of the physical bandwidth is completely unnecessary. In the next section, the author investigates the effect of various parameters of power-saving routers and Pathload on their behaviors and reveals the conditions on which the power-saving router change its physical bandwidth due to measurement traffic load.



(a) Physical bandwidth does not change



(b) Physical bandwidth changes in the first measurement process

Figure 1: Measurement process of Pathload

3 Performance evaluation of Pathload with a power-saving router

In this section, the performance of Pathload in the environment with power-saving routers whose behaviors are defined in the previous section is evaluated, by conducting simulation experiments with ns-2 network simulator [40]. Both of the energy efficiency of the power-saving router and the measurement accuracy of Pathload are evaluated.

3.1 Simulation settings

Figure 2 depicts the network topology used in the simulation experiments. It is assumed that a *power-saving router* is connected to a *tight link*, which provides the narrowest bandwidth along the network path between a *sender* and a *receiver*. The maximum physical bandwidth of the tight link is denoted as C_{max} . Other links, labeled as *normal links* in the figure, provide sufficiently large physical link bandwidth, which is twice as wide as the tight-link bandwidth. The propagation delay of each link is 5 ms. Cross traffic which traverses the tight link is generated from a *cross traffic sender* to a *cross traffic receiver*. The load of the cross traffic is set to 10% of C_{max} .

With these settings, the measurement of the available bandwidth by Pathload is conducted for the path between the sender and the receiver. Table 1 summarizes other parameters of the power-saving router, and the parameters for Pathload are shown in Table 2. The total time of each simulation experiment is 100 s. A Pathload measurement is conducted every 10 s, starting at 60 s, and cross traffic is injected from the beginning of the simulation experiments. The initial value of the physical link bandwidth of the power-saving router is set to C_{max} . Therefore, at the beginning of the simulation experiments, the power-saving router gradually decreases its physical bandwidth according to the amount of cross traffic.

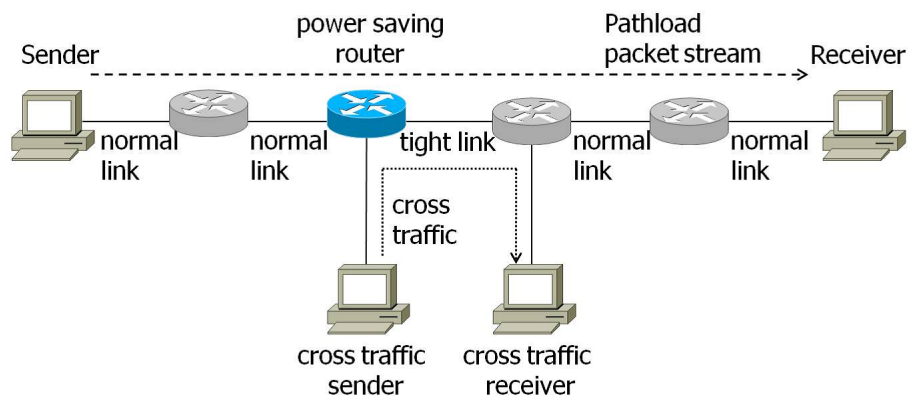


Figure 2: Network topology for simulation experiments

Table 1: Parameters of power-saving router

Parameter	Variable	Value
Maximum value of physical link bandwidth	C_{max}	2000 Mbps, 1000 Mbps, 100 Mbps, 10 Mbps
Number of steps for regulating physical bandwidth	N	10
Upper threshold of link utilization for increasing physical bandwidth	λ_u	0.8
Lower threshold of link utilization for decreasing physical bandwidth	λ_l	0.3
Averaging weight	w	0.3
Length of the interval for monitoring link utilization	τ	100 , 10 , 5, 1 ms

Table 2: Parameters of Pathload

Parameter	Value
Probing packet size	1500 bytes
Number of packets included in a packet stream	25
Number of streams for determining the trend	3
Estimate resolution	1 Mbps

3.2 Behavior of the power-saving router

First, the author focuses on the impact of traffic generated by Pathload on the physical bandwidth of the power-saving router. C_{max} is set to 100 Mbps and τ is changed as 100 ms, 10 ms, 5 ms and 1 ms. In Figures 3 and 4, the changes in the average link utilization and those in the physical link bandwidth are plotted, respectively, as functions of the simulation time.

These figures indicate that regardless of the value of τ , the physical link bandwidth and the link utilization converge to 20 Mbps and 0.5, respectively, before Pathload starts the measurement at 60 s. These results are from the fact that the power-saving router decreases its physical link bandwidth in order to reduce power consumption. In addition, Figure 3 shows that the link utilization temporarily increases when Pathload starts measuring the available bandwidth. Specifically, the link utilization increases largely when using small τ . Furthermore, when $\tau = 5$ ms or 1 ms, the power-saving router increases its physical link bandwidth when the measurement starts, as seen in Figures 4(c) and 4(d). In particular, when $\tau = 5$ ms, the physical link bandwidth increases to 30 Mbps even after the end of the bandwidth measurement. These results clearly demonstrate the adverse effect of bandwidth measurement traffic on the energy efficiency of power-saving routers.

These behaviors of the power-saving router are due to the SLoPS algorithm commonly utilized by bandwidth measurement tools, including Pathload. When bandwidth measurement is performed with SLoPS, multiple packets are injected into the network to fill the available/physical bandwidth at the bottleneck link. This procedure increases the utilization of the tight link bandwidth, which in turn causes the power-saving router to increase its physical bandwidth. The differences in the behavior of the router at different values of τ are caused by the algorithm utilized by Pathload, where the sender injects multiple packet streams, each of which consists of multiple packets, into the network at a certain intervals.

Next, the behavior of the power-saving router is observed when $\tau = 5$ ms and the value of C_{max} is varied. Figures 5 and 6 show the changes in link utilization and physical link bandwidth of the power-saving router as functions of the simulation time when C_{max} is set to 2000 Mbps, 1000 Mbps, 100 Mbps, and 10 Mbps. It can be seen from Figure 5 that the change in link utilization becomes large when C_{max} becomes small. In addition, from Figure 6, it can be observed that although the power-saving router does not increase its physical bandwidth during measurements

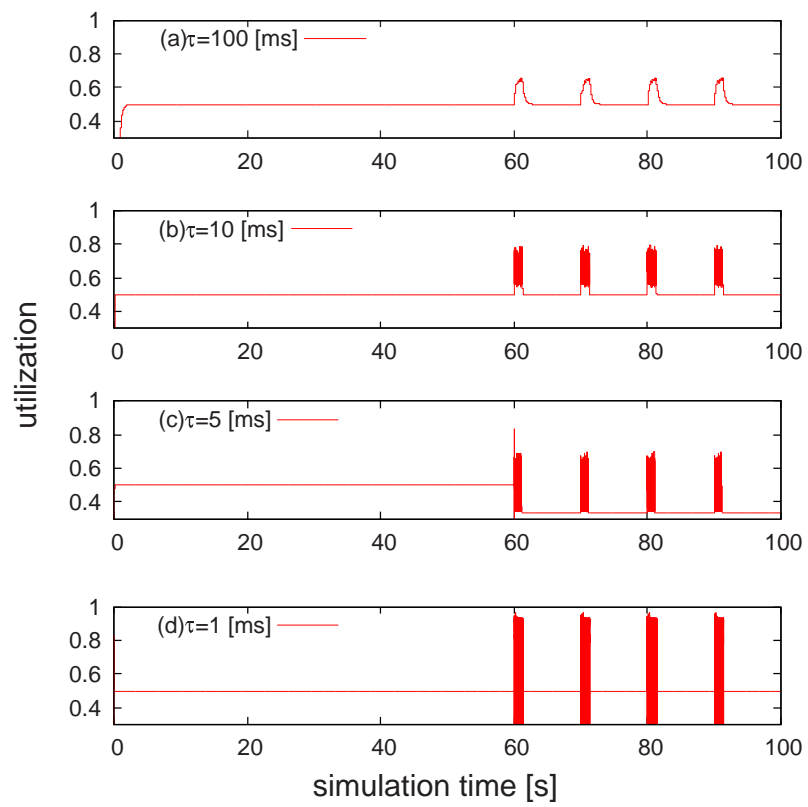


Figure 3: Change in the utilization of the tight link

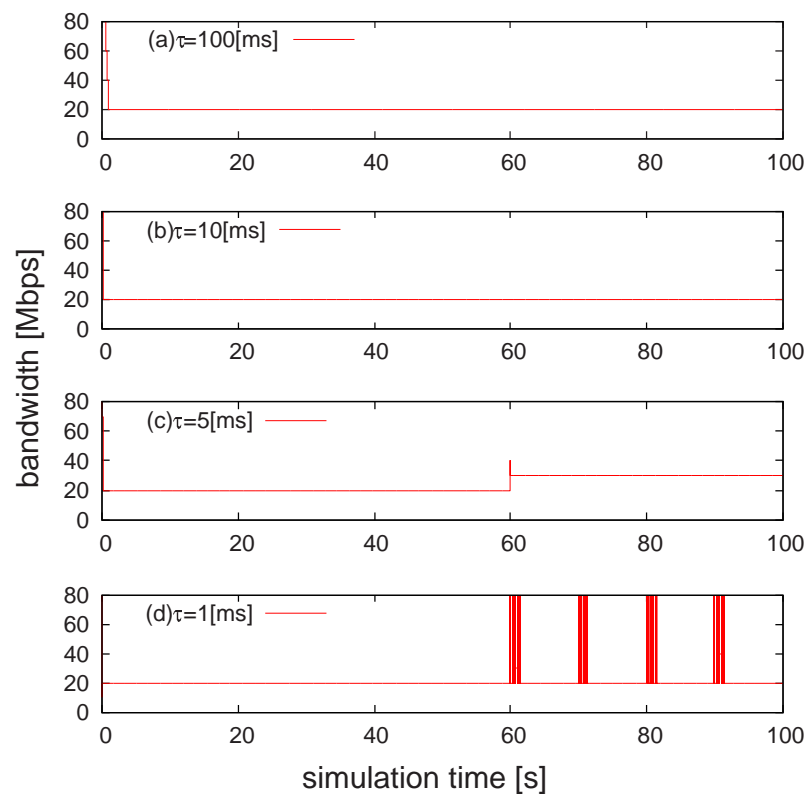


Figure 4: Change in the physical bandwidth of the tight link

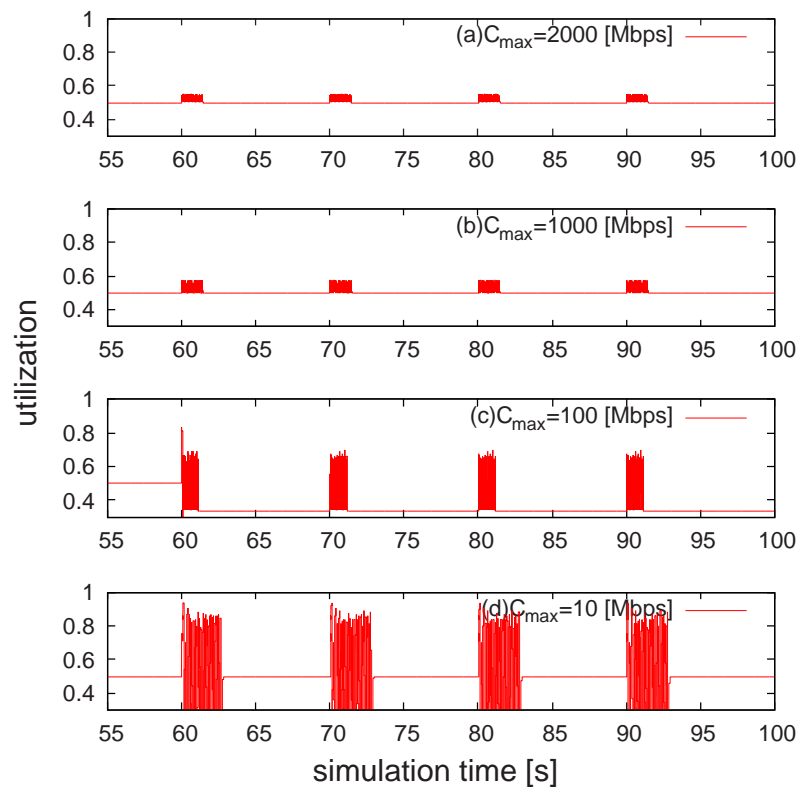


Figure 5: Effect of the maximum bandwidth of the tight link on the utilization changes

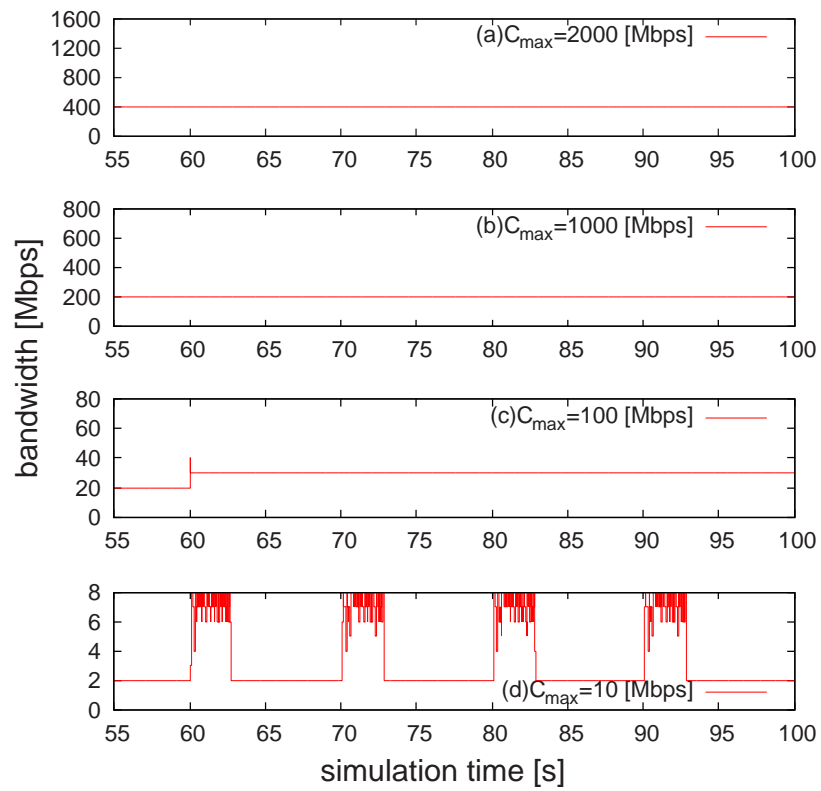


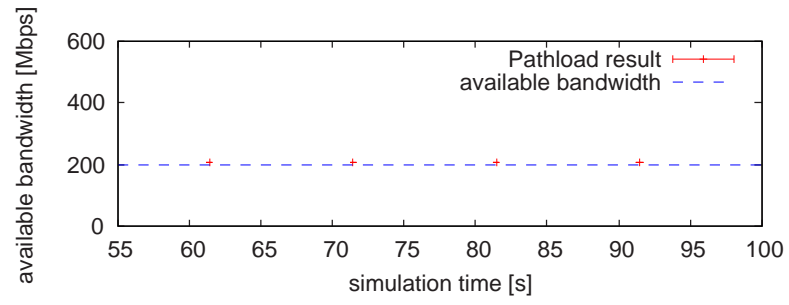
Figure 6: Effect of the maximum bandwidth of the tight link on the physical bandwidth changes

when C_{max} is 2000 Mbps or 1000 Mbps, it does when $C_{max} = 100$ Mbps or 10 Mbps. This behavior of the power-saving router can be explained as in Subsection 2.3. In Figures 5(a), 5(b), 5(c), and 5(d), the available bandwidth at 60 s, which is the time of starting measurement, are 200 Mbps, 100 Mbps, 10 Mbps, and 1 Mbps, respectively. When $C_{max} = 100$ Mbps or 10 Mbps, the available bandwidth is smaller than the other cases. Therefore, it is considered that the effect of Pathload's measurement on the power-saving router is large in these situations.

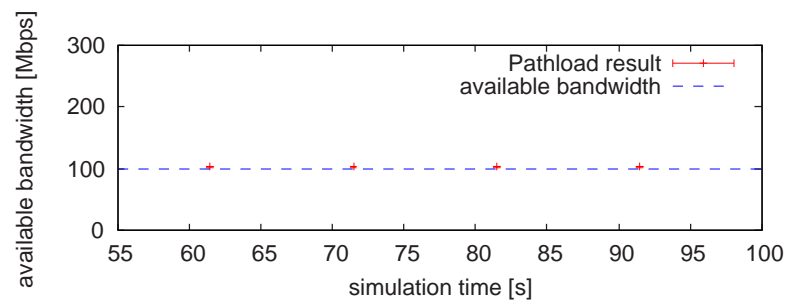
3.3 Measurement accuracy of Pathload

Here, the author evaluates the measurement accuracy of Pathload in the presence of a power-saving router. In Figures 7(a), 7(b), 7(c), and 7(d), the measurement results by Pathload is plotted when $C_{max} = 2000$ Mbps, 1000 Mbps, 100 Mbps, and 10 Mbps, respectively. The available bandwidth before the measurement is shown together with the Pathload results with error bars since Pathload gives the measurement results as a range of possible values for the available bandwidth.

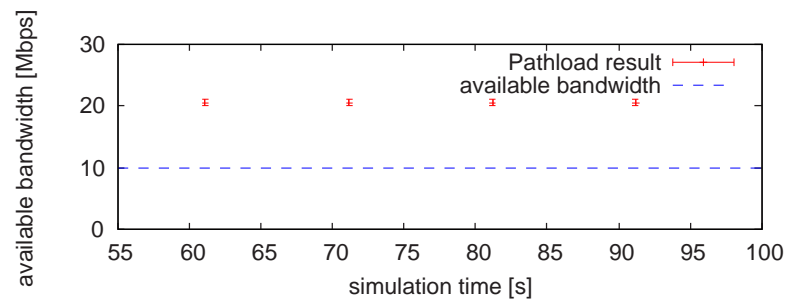
Figures 7(a) and 7(b) show that the measurement results obtained with Pathload include the true available bandwidth. This follows from the fact that the physical bandwidth does not change when Pathload starts the measurement, as shown in Figures 6(a) and 6(b). However, Figures 7(c) and 7(d) show that the results obtained with Pathload are far from the true available bandwidth in the cases of $C_{max} = 100$ Mbps and 10 Mbps since the power-saving router increased its physical link bandwidth due to the measurement load caused by Pathload, as shown in Figure 6(c) and 6(d). These results indicate that the behavior of the power-saving router degrades the measurement accuracy for the end-to-end available bandwidth.



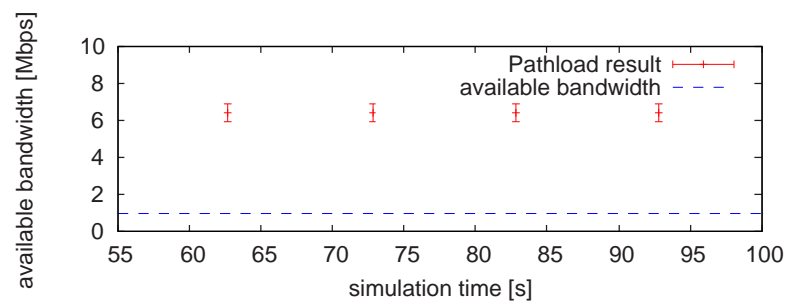
(a) $C_{max} = 2000$ Mbps



(b) $C_{max} = 1000$ Mbps



(c) $C_{max} = 100$ Mbps



(d) $C_{max} = 10$ Mbps

Figure 7: Measurement results obtained with Pathload

4 Parameter tuning of Pathload for not affecting a power-saving router

In Section 3, the author indicated that Pathload is unable to measure the available bandwidth accurately when the power-saving router increases its physical bandwidth to accommodate the measurement load caused by Pathload. It should be also noted that the changes in the physical bandwidth of the power-saving router degrades its energy efficiency. In this section, the author discusses the parameter tuning of Pathload which ensure that the behavior of the power-saving router remains unaffected during the measurement, through simple mathematical analysis.

4.1 Conditions for not affecting a power-saving router

It is assumed that the power-saving router has already configured its physical bandwidth according to the current traffic load. Using Equations (3) and (4), the conditions for the power-saving router to maintain its physical bandwidth are as follows.

$$\begin{aligned} U(t) &= (1 - w)U(t - 1) + wu(t) \\ &= w \sum_{k=1}^t (1 - w)^{t-k} u(k) \\ &\leq \lambda_u \end{aligned} \tag{8}$$

$P(t)$, which is the amount of traffic observed at the tight link, is divided into $P^L(t)$ and $P^C(t)$ as follows.

$$P(t) = P^L(t) + P^C(t) \tag{9}$$

where $P^L(t)$ represents the amount of traffic caused by Pathload while measuring the available bandwidth which arrives at the tight link at the t th time slot, and $P^C(t)$ is the amount of cross traffic. By using Equations (2), (3) and (9), the average link utilization $U(t)$ can be rewritten as

follows.

$$\begin{aligned}
U(t) &= w \sum_{k=1}^t (1-w)^{t-k} u(k) \\
&= w \sum_{k=1}^t (1-w)^{t-k} \frac{P^L(k) + P^C(k)}{C(t)\tau} \\
&= w \sum_{k=1}^t (1-w)^{t-k} \frac{P^L(k)}{C(t)\tau} + \\
&\quad w \sum_{k=1}^t (1-w)^{t-k} \frac{P^C(k)}{C(t)\tau}
\end{aligned} \tag{10}$$

The first term in Equation (10) represents traffic contributed by Pathload while measuring the link utilization, and the second term represents cross traffic. Assuming cross traffic arriving at the tight link at a fixed rate R^C , Equation (10) can be rewritten as follows.

$$U(t) = w \sum_{k=1}^t (1-w)^{t-k} \frac{P^L(k)}{C(t)\tau} + \frac{R^C}{C(t)} \tag{11}$$

In the following discussion, it is assumed $\tau \leq V_S(f)$, in other words, a utilization monitoring interval is shorter than the length of the packet stream sent by Pathload since in such cases the measurement traffic generated by Pathload strongly influences the behavior of power-saving routers. For simplicity, it is assumed $V_S(f) = j\tau$, where j is an integer greater than one. The relationship between packet stream length and monitoring interval is presented in Figure 8, where the power-saving router monitors the probing packet stream for time slots t_0, t_1, \dots, t_{j-1} . Since the arrival rate of packet streams is close to the available bandwidth, the link utilization increases considerably, particularly when the packet stream spans multiple monitoring intervals of link utilization, which are denoted as time slots t_0, \dots, t_{j-1} in Figure 8. In this situation, Equation (8) can be rewritten based on Equation (11), assuming that the interval between two packet streams is sufficiently large not to affect the calculation of average link utilization in Equation (3).

$$\begin{aligned}
U(t_{j-1}) &= w \sum_{k=0}^{j-1} (1-w)^{j-1-k} \frac{R(f)}{C(t)} + \frac{R^C}{C(t)} \\
&\leq \lambda_u
\end{aligned} \tag{12}$$

Note that only j can be controlled to satisfy Equation (12), which is achieved by changing K (the number of packets contained in the packet stream). Therefore, by configuring the number of packets in each packet stream to satisfy Equation (12), we can prevent Pathload from affecting the behavior of power-saving routers.

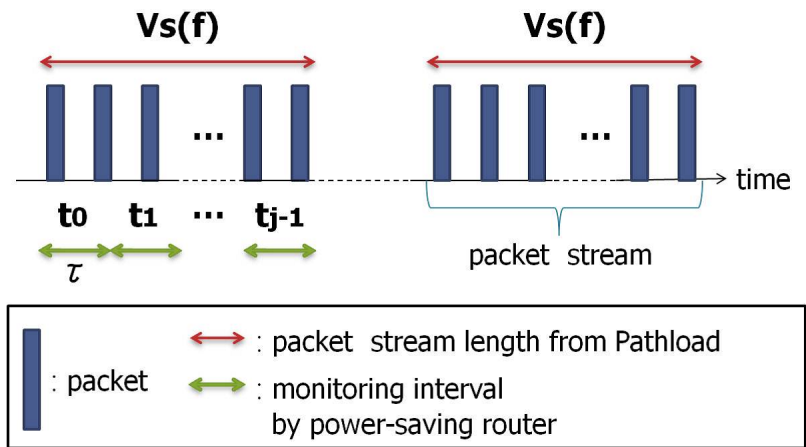


Figure 8: Relationship between packet stream length and monitoring interval

4.2 Verification

The author verifies the validity of Equation (12) through comparison with the simulation results in Figures 3 and 4. Specifically, Figures 3(b), 3(c), and 3(d), and Figures 4(b), 4(c), and 4(d) to assess Equation (12) are utilized because of the constraint of $\tau \leq V_S(f)$. The highest rate of packet streams in the simulation is assumed the value of $R(f)$, which is 16 Mbps. In this case, $U(t)$ in Equation (12) becomes 0.74, 0.91 and 1.28 when τ is 10 ms, 5 ms and 1 ms, respectively. Since λ_u is 0.8, an increase in the physical bandwidth is expected when τ is set to 5 ms or 1 ms. Figure 4 confirms the expectation that the physical bandwidth remains unchanged only for $\tau = 10$ ms in Figure 4(b), while the physical bandwidth increases when the measurement is started, as shown in Figures 4(c) and 4(d) with $\tau = 5$ ms and 1 ms, respectively.

For ensuring these results in more detail, the author conducted the additional simulation experiments where the number of probe packets per packet stream is changed. Here, C_{max} and τ are set to 100 Mbps and 5 ms, respectively. Figures 9 and 10 show that the changes in the link utilization and physical bandwidth of the power-saving router, respectively, when K is set to 50, 25, and 12. $U(t)$ in Equation (12) becomes 1.11, 0.91, and 0.74 when K is 50, 25, and 12, respectively. When K is set to 50 or 25, an increase in the physical bandwidth is expected, since λ_u is 0.8. Figures 10(a) and 10(b) indicate that this expectation is true. Furthermore, Figure 10(c) confirms the expectation that the physical bandwidth remains unchanged.

The above results confirm the validity of Equation (12) in terms of providing the conditions where the energy efficiency of power-saving routers remains unaffected.

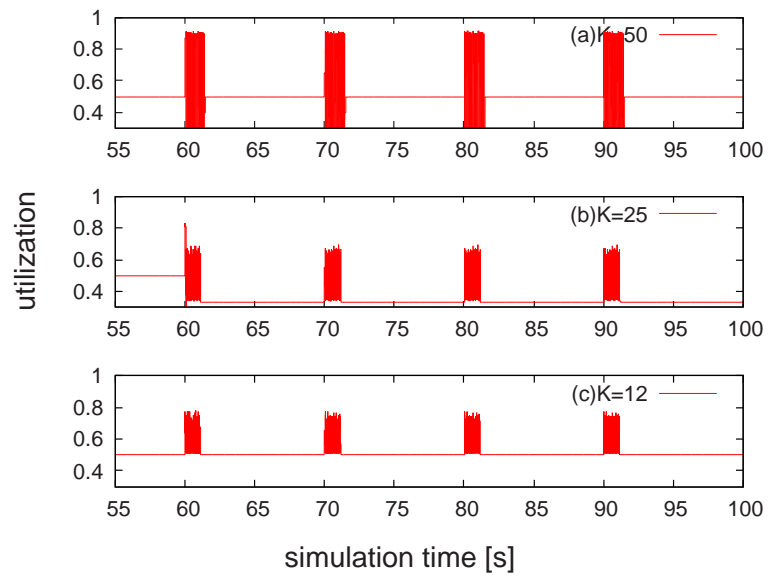


Figure 9: Effect of the number of packets of per packet stream on the utilization changes

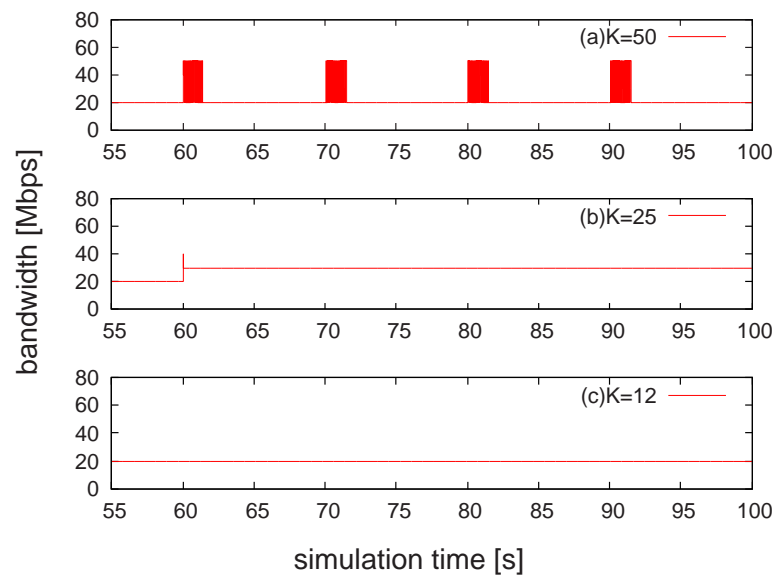


Figure 10: Effect of the number of packets of per packet stream on the physical bandwidth changes

5 Conclusions and future works

In this thesis, the author described a parameter tuning method for Pathload to maintain the measurement accuracy in the network with power-saving routers, while not affecting the behavior of power-saving routers. The author first investigated the interactions between the bandwidth measurement behavior of Pathload and the energy efficiency of power-saving routers by conducting extensive simulation experiments. The simulation results indicated that both the measurement accuracy of Pathload and the energy efficiency of power-saving routers would degrade, particularly when the power saving functions were triggered in short cycles or when the available bandwidth of the power-saving router was small. The author also showed that Pathload can measure an available bandwidth without affecting the behavior of power-saving routers by tuning the number of probing packets on the basis of the mathematical analysis results.

In future work, the author plans to evaluate the measurement accuracy of Pathload after parameter tuning. The author also plans to enhance the algorithm of Pathload to accommodate power-saving routers by implementing an automatic parameter tuning to avoid the adverse effects of traffic generated by Pathload on the energy efficiency of power-saving routers. It is also a future task to enable the measurement of available bandwidth based on the maximum physical link bandwidth of power-saving routers regardless of power-saving router's condition. The next step is to propose and evaluation a new transport protocol which uses information of end-to-end available bandwidth as a congestion indicator.

Acknowledgement

The author appreciates people who related with my research.

First, the author would like to express my gratitude to Professor Hirotaka Nakano of Osaka University. His advices have brought significant advances in my research. The author also appreciates Professor Masayuki Murata of Osaka University. He has led me proper appreciation of not only my research but also my career. The author would like to convey my gratitude to Professor Go Hasegawa of Osaka University. His guidance has significantly helped me progress as a researcher. The author is grateful to Assistant Professor Yoshiaki Taniguchi of Osaka University for his supporting my research and life of Nakano Laboratory. The author also thanks colleagues at Nakano Laboratory. Finally, the author would like to express my thankfulness to my family for warmly following my life.

References

- [1] METI, “Green IT Initiative in Japan,” 2008. available at <http://www.meti.go.jp/english/policy/GreenITInitiativeInJapan.pdf>.
- [2] R. Kubo, J. Kani, H. Ujikawa, Y. Fujimoto, N. Yoshimoto, and H. Hadama, “Study and demonstration of sleep and adaptive link rate control mechanisms for energy efficient 10G-EPON,” *IEEE/OSA Journal of Optical Communications and Networking*, vol. 2, no. 9, pp. 716–729, September 2010.
- [3] F. Blanquicet and K. Christensen, “An initial performance evaluation of rapid PHY selection (RPS) for energy efficient ethernet,” in *Proceedings of the 32nd IEEE Conference on Local Computer Networks*, pp. 223–225, October 2007.
- [4] G. Ginis, “Low-power modes for ADSL2 and ADSL2+.” White paper, Broadband Communications Group, Texas Instruments, January 2005.
- [5] K. Kotla and A. Reddy, “Making a delay-based protocol adaptive to heterogeneous environments,” in *Proceedings of the 16th International Workshop on Quality of Service. 16th International Workshop*, pp. 100–109, June 2008.
- [6] E. Gamess, P. Marrero, and D. Gámez, “A delay based routing protocol with support for common services,” in *Proceedings of the 6th Latin America Networking Conference*, pp. 64–73, October 2011.
- [7] Y. Chan, C. Lin, and F. Liu, “A competitive delay-based TCP,” in *Proceedings of Research, Innovation and Vision for the Future*, pp. 134–140, July 2008.
- [8] L. Vicisano, J. Crowcroft, and L. Rizzo, “TCP-like congestion control for layered multicast data transfer,” in *Proceedings of INFOCOM’98*, pp. 996–1003, March 1998.
- [9] S. Liu, T. Basar, and R. Srikant, “TCP-Illinois: A loss- and delay-based congestion control algorithm for high-speed networks,” *Performance Evaluation*, vol. 65, no. 6-7, pp. 417–440, June 2008.

- [10] D. X. Wei, C. Jin, S. H. Low, and S. Hegde, "FAST TCP: Motivation, architecture, algorithms, performance," *IEEE/ACM Transactions on Networking*, vol. 14, no. 6, pp. 1246 – 1259, December 2006.
- [11] D. Hayes and G. Armitage, "Improved coexistence and loss tolerance for delay based TCP congestion control," in *Proceedings of Local Computer Networks (LCN)*, pp. 24–31, October 2010.
- [12] Y. Chen, D. Bindel, H. Song, and R. H. Katz, "An algebraic approach to practical and scalable overlay network monitoring," in *Proceedings of ACM SIGCOMM 2004*, pp. 55–66, August 2004.
- [13] Cisco NetFlow, available at http://www.cisco.com/application/pdf/en/us/guest/tech/tk812/c1482/ccmigration_09186a00802de684.pdf.
- [14] MRTG Web site, available at <http://oss.oetiker.ch/mrtg/>.
- [15] N. Hu and P. Steenkiste, "Exploiting internet route sharing for large scale available bandwidth estimation," in *Proceedings of IMC 2005*, pp. 16–20, October 2005.
- [16] D. Sisalem and F. Emanuel, "QoS control using adaptive layered data transmission," in *Proceedings of Multimedia Computing and Systems*, pp. 4–12, June 1998.
- [17] J. Postel, "RFC793-transmission control protocol," September 1981.
- [18] I. Rhee and L. Xu, "CUBIC: A new TCP-friendly high-speed TCP variant," in *Proceedings of PFLDnet 2005*, February 2005.
- [19] K. Tan, J. Song, and M. Sridharan, "A Compound TCP Approach for High-speed and Long Distance Networks," tech. rep., Microsoft Research, July 2005.
- [20] T. Iguchi, G. Hasegawa, and M. Murata, "A new congestion control mechanism of TCP with inline network measurement," in *Proceedings of ICOIN2005*, January 2005.
- [21] G. Hasegawa and M. Murata, "TCP symbiosis: congestion control mechanisms of TCP based on Lotka-Volterra competition model," in *Proceedings of Workshop on interdisciplinary systems approach in performance evaluation and design of computer & communications systems (Inter-Perf 2006)*, October 2006.

- [22] M. Jain and C. Dovrolis, “End-to-end available bandwidth: Measurement methodology, dynamics, and relation with TCP throughput,” in *Proceedings of ACM SIGCOMM 2002*, pp. 295–308, July 2002.
- [23] C. L. T. Man, G. Hasegawa, and M. Murata, “ImTCP: TCP with an inline measurement mechanism for available bandwidth,” *Computer Communications Journal special issue of Monitoring and Measurements of IP Networks*, vol. 29, no. 10, pp. 2469–2479, June 2006.
- [24] V. J. Ribeiro, R. H. Riedi, R. G. Baraniuk, J. Navratil, and L. Cottrell, “pathChirp: Efficient available bandwidth estimation for network paths,” in *Proceedings of Passive and Active Measurements (PAM 2003) Workshop*, pp. 1–11, April 2003.
- [25] J. Strauss, D. Katabi, and F. Kaashoek, “A measurement study of available bandwidth estimation tools,” in *Proceedings of the 3rd ACM SIGCOMM conference on Internet measurement*, pp. 39–44, October 2003.
- [26] A. Downey, “Using pathchar to estimate Internet link characteristics,” in *Proceedings of ACM SIGCOMM 1999*, pp. 241–250, October 1999.
- [27] N. Hu and P. Steenkiste, “Evaluation and characterization of available bandwidth probing techniques,” *IEEE Journal on Selected Areas in Communications*, vol. 21, no. 6, pp. 879–894, August 2003.
- [28] J. Navratil and R. L. Cottrell, “ABwE: A practical approach to available bandwidth estimation,” in *Proceedings of Passive and Active Measurements (PAM 2003) Workshop*, April 2003.
- [29] E. Bergfeldt, S. Ekelin, and J. M. Karlsson, “Real-time available-bandwidth estimation using filtering and change detection,” *Computer Networks: The International Journal of Computer and Telecommunications Networking*, vol. 53, no. 15, pp. 2617–2645, October 2009.
- [30] M. Jain and C. Dovrolis, “End-to-end estimation of the available bandwidth variation range,” in *Proceedings of the 2005 ACM SIGMETRICS international conference on Measurement and modeling of computer systems*, pp. 265–276, June 2005.

- [31] L. Lao, C. Dovrolis, and M. Y. Sanadidi, “The probe gap model can underestimate the available bandwidth of multihop paths,” *ACM SIGCOMM Computer Communication*, vol. 36, pp. 29–34, October 2006.
- [32] X. Hei, B. Bensaou, and D. H. K. Tsang, “Model-based end-to-end available bandwidth inference using queueing analysis,” *Computer Networks: The International Journal of Computer and Telecommunications Networking*, vol. 50, no. 12, pp. 1916–1937, August 2006.
- [33] C. L. T. Man, G. Hasegawa, and M. Murata, “ICIM: An inline network measurement mechanism for highspeed networks,” in *Proceedings of the E2EMON Workshop 2006*, pp. 66 – 73, April 2006.
- [34] Pchar. available at <http://www.kitchenlab.org/www/bmah/Software/pchar/>.
- [35] Pathchar. available at <http://www.caida.org/tools/utilities/others/pathchar/>.
- [36] A. Shriram, M. Murray, Y. Hyun, N. Brownlee, A. Broido, M. Fomenkov, and K. claffy, “Comparison of public end-to-end bandwidth estimation tools on high-speed links,” in *Proceedings of Passive and Active Measurements (PAM 2005) Workshop*, pp. 306–320, March 2005.
- [37] T. Chiping and M. Philip, “On the cost-quality tradeoff in topology-aware overlay path probing,” in *Proceedings of the 11th IEEE International Conference on Network Protocols*, pp. 268–279, November 2003.
- [38] S. Ata, K. Yonezaki, and I. Oka, “A method of traffic prediction for performance adjustable energy-aware routers,” *IEICE technical report*, vol. 111, no. 43, pp. 121–126, May 2011. (in Japanese).
- [39] M. Jain and C. Dovrolis, “Pathload: A measurement tool for End-to-End available bandwidth,” in *Proceedings of Passive and Active Measurements (PAM 2002) Workshop*, pp. 14–25, March 2002.
- [40] The VINT Project, “UCB/LBNL/VINT network simulator - ns (version 2).”